COMPUTATIONAL THREE DIMENSIONAL SIMULATION OF THE FLOW WITHIN PROGRESSING CAVITY PUMPS

Emilio E. Paladino, emilio@dem.ufrn.br
João A. de Lima, jalima@dem.ufrn.br
Department of Mechanical Engineering, Federal University of Rio Grande do Norte, CEP 59072-970- Natal - RN

Paulo A. S. Pessoa, pauloalison@msn.com
Rairam F. C. Almeida, rairamalmeida@gmail.com
PPGEM - Graduate Program in Mechanical Engineering, Federal University of Rio Grande do Norte, CEP 59072-970- Natal - RN

Abstract. *This work presents a novel computational model for the 3D flow in a Progressing Cavity Pump (PCP) which includes the relative motion between rotor and stator. The governing equations are solved using an element based finite volume method in a moving mesh. The model developed is capable of the accurate prediction of volumetric efficiency and viscous looses as well as provide detailed information of pressure and velocity fields inside this device. This could allow the prediction of local stator deformation, trough fluid-structure interaction approach, in order to predict how this influences the flow and, ultimately, the pump performance. In addition, turbulence effects can be accurately treated, by using advanced turbulence models and the model can be extended for the case of multiphase flows, which is a common case in artificial lift systems. The results hereby presented, consider a rigid stator pump. The model was validated against experimental results from literature. Results showed to be fairly sensitive to the mesh size, then a grid refinement study is presented. In addition, some aspects related to the dynamic behavior of the flow, not captured by the simplified models, are analyzed using this model.*

Keywords*: Artificial lift, pumps, PCP, CFD*

1. INTRODUCTION

The use of Progressing Cavity Pumps -PCPs- in downhole pumping applications in low deep wells is becoming more common replacing, in some cases, the traditional reciprocating pumps. Among the main advantages of this system the ability to pump heavy oils, produce large concentrations of sand, tolerate high percentages of free gas and high efficiency, can be quoted. The growth of this system as artificial lift system in the last years lead to the need of the development of more accurate flow models within these devices. As any positive displacement pump, the basic idea is to "displace" the fluid from a low pressure to high pressure regions and seals are needed between moving and static parts, in order to avoid the counterflow (from high to low pressure regions). The detailed understanding of flow behavior within Progressing Cavity Pumps is of fundamental importance for PCP artificial lift systems design, optimization and operation. Operational cost reduction, life extension (wear reduction) and increase in oil production can be mentioned among the benefits of this knowledge.

This work presents a computational model for the unsteady 3D flow, using an Element Based Finite Volume Method (Baliga & Patankar, 1980; Raw, 1985; Maliska, 2004), which includes the relative motion between rotor and stator, in Progressing Cavity Pumps. Full 3D velocity fields are obtained from the model, together with pressure field. Then, all flow variables, including flow rate, torque, efficiency, etc. can be evaluated. It is worthwhile to mention that this model intends to be an additional tool for PCP systems design and operation and not substitute experimentation or pilot/in-field testing. Nevertheless, experimentation is expensive and it is difficult to obtain local measurements of pressure and velocity fields. In addition, real operational conditions, as downhole pressures and temperatures are difficult (sometimes, impossible) to reproduce in laboratory tests, but can easily studied though the computational model hereby presented. Once the model is validated through experiments developed under laboratory realizable conditions, the computational model can be used for other operational conditions.

Based on the ideas of the system creator, Rene Moineau (Moineau, 1930), usual flow models attempt to establish relations between differential pressure and flow rate by subtracting the counterflow leaked from seals, from the displaced flow rate. As the displaced flow rate depends only on pump geometry and kinematics, fluid models usually attempt to calculate the leakage or "slippage"[1], which is function of pump geometry, fluid properties and differential pressure along the pump. As differential pressure increases, so does the slippage, and the relation between differential pressure across the pump and net volumetric flow pumped, can be calculated. Still, although several works related to the PCP application and control in artificial lift systems were published, few references were encountered aiming the flow characterization within PCPs. Robello & Saveth (1998) developed optimal relationships between the pitch and the diameter of the stator to achieve a maximum flow rate for multilobe pumps. This work is focused on pump geometrical parameters and their influence on displaced flow rate, but no mention is done to the slippage, and so on the influence of differential pressure on pumped flow rate. Olivet *et al.* (2002) performed an experimental study in PCPs for single- and

[1] This term is commonly used in PCP and screw pumps terminology, as fluid is displaced axially through the pump, and counterflow "slips" over the displaced flow.

two-phase flow conditions and obtained characteristic curves and transient pressure profiles within cavities in metallic (rigid) stator pumps.

Gamboa *et al.* (2002) presented some attempts of flow modeling within a PCP using Computational Fluid Dynamics with the aim of getting a better comprehension of the flow inside the pump. Nevertheless, attempts for developing a three-dimensional model including rotor motion failed due to the complexity of the geometry, mesh motion and (maybe) the inadequateness or limitations of the numerical approach used to solve the governing equations. In virtue of this, Gamboa *et al.* (2003) presented a simplified model for single phase flow considering the possibility of variable gap due to elastomeric stator deformation. The model is similar to presented in other works, based on the aforementioned Moineau's approach, but the slippage is calculated considering the possibility of a variation of the clearance as function of differential pressure. In this way they were able to reproduce the characteristic non-linear behavior of volumetric flow versus differential pressure in a PCP with elastomeric stator. Another interesting model was presented in Andrade (2008) who solved the flow within a "developed" pump, i.e., the flow was solved between two plates, which local separation corresponds to the distance between rotor and stator, using a an approach similar to the lubrication theory, where the inertial terms are neglected in transport equations but transient term is retained. This approach presents good results for viscous fluids, but it is not suitable for low viscosity fluids where inertial terms become important and flow can eventually become turbulent.

Nevertheless, after an extensive literature review, no flow models considering the solution for the full transient 3D Navier-Stokes equations and relative motion rotor and stator were found. The accurate treatment of turbulence effects through advanced turbulence models, account of variation of fluid properties, with temperature and pressure and the capability to be extended for multiphase flow case, can be cited among the several advantages of the model presented in this work.

1.1 PCP operation principle and performance curves

This section aims to briefly describe the operational principle of PCPs, in order to understand the shortcomings of the flow modeling and expected results. However, a detailed explanation of PCPs design and operation is beyond the scope of this paper and can be encountered, for instance, in Nelik & Brennan (2005), ISO (2008) and other references.

Progressing Cavity Pumps are positive displacement pumps similar to screw pumps but, in this case, the fluid displacement is promoted trough and eccentric motion of a rotor (that's because these pumps are also called "eccentric screw pump").

The cavities are isolated through the seal lines, as shown in Figure 1, and the fluid within them is displaced from low to high pressure regions. As total differential pressure increases, the pump length, and so the number of cavities, need to be increased in order to reduce the differential pressure between adjacent cavities, reducing the slippage.

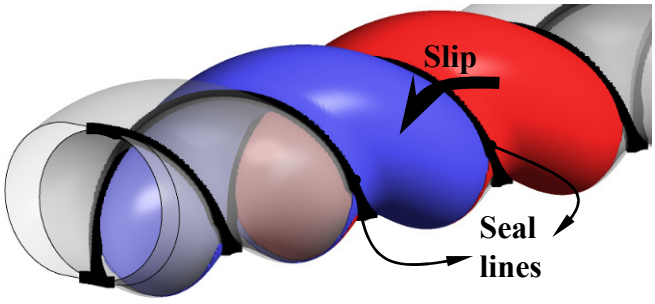

Figure 1. Cavities and seal lines in a PCP

The seal is done trough a very fine channel between cavities. Depending on the pump type there could be an interference between rotor and stator or a clearance, as shown in Figure 2. For the case of interference between rotor and stator, a non rigid (elastomeric) stator is used, in order to allow the deformation imposed by the rotor motion. In this case, the seal is tight and the slippage is almost zero. Nevertheless, it can considered that, at regular operation, a fine liquid film is present between rotor and stator, even in the case of interference. This hypothesis is important in terms of flow modeling, as a single connected domain can be employed. For the case with interference a very fine channel between rotor and stator was considered in computational model as shown in Figure 6.

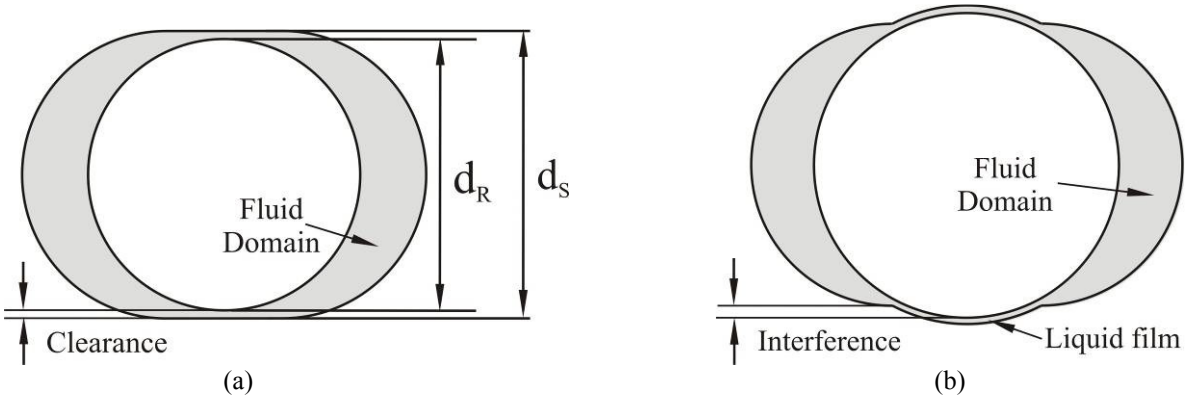

Figure 2. Axial view of fluid domains considered in for metallic (a) and elastomeric (b) stator PCPs and main geometrical parameters (liquid film is out of scale)

As stated previously, the volumetric flow rate can be calculated as the volume displaced in each revolution multiplied by the rotation (which is called "theoretical flow rate") and subtracting the leaked flow across the seal regions.

Several factors affect the slippage: The clearance between rotor and stator, fluid viscosity and pressure drop between cavities (which depends on the pressure drop along the whole pump), among others. Figure 3 shows schematically the typical shape of performance curves for elastomeric and metallic stator. For the case of elastomeric stator, the pump operates with interference between rotor and stator and, for operation at relatively low pressures, the cavities are maintained almost enclosed and the pumped flow rate is equal to the displaced flow rate. Nevertheless, once the stator is deformable, as pressure is increased, so does the deformation and the slippage between cavities. When the deformation exceeds the interference, the slippage increases more significantly (not linearly, as the clearance is variable) with pressure drop. For the metallic stator case, the pump is designed to operate with a clearance between rotor and stator which is constant as the stator deformation is negligible for usual pressures levels. As will be seen in results section, for high viscosity fluids the flow along the sealing regions is laminar, and slippage varies linearly with pressure drop for rigid stator. For turbulent flow case, the slippage will be proportional to some power (n<1) of pressure drop and the pumped flow rate will vary non linearly with pressure difference along the pump.

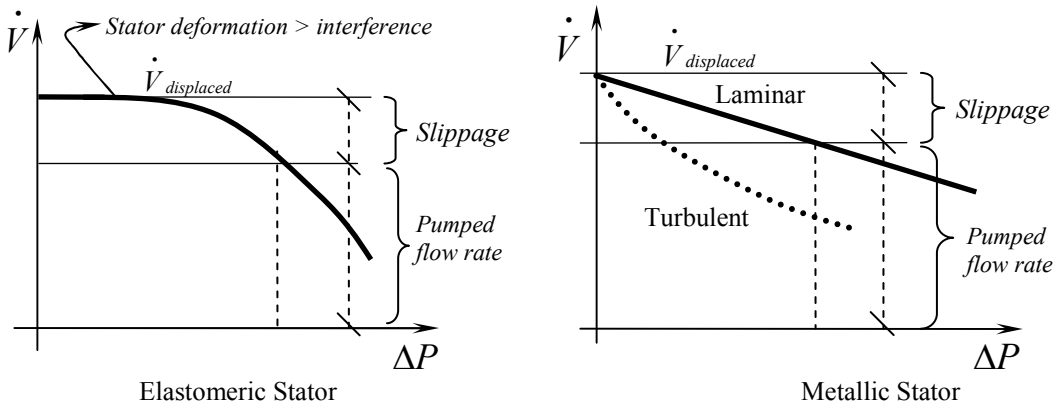

Figure 3. Expected characteristic curves for metallic (a) and elastomeric (b) stator PCPs

2. COMPUTATIONAL MODEL

The computational model for the flow in a Progressing Cavity Pump was implemented in CFX11 (ANSYS, 2008). This software is based on a discretization of the governing equations using and Element Based Finite Volume Method (Baliga & Patankar, 1980); Ferziger & Peric, 2001; Maliska, 2004) and a coupled approach for solving the pressure-velocity decoupling (Raw (1985)).

The flow was solved as incompressible and isothermal. In field applications will certainly comprise multiphase flow with variable thermodynamic and transport properties but, for the sake of simplicity, the model was implemented, initially, only for a liquid phase, and then only mass and momentum conservation equations,

$$\frac{\partial \rho}{\partial t} + \nabla \cdot (\rho \mathbf{V}) = 0 \tag{1}$$

$$\frac{\partial \rho \mathbf{V}}{\partial t} + \nabla \cdot (\rho \mathbf{V}\mathbf{V}) = -\nabla \cdot p + \nabla \cdot \left(\mathbf{T} + \mathbf{T}^{Turb}\right) \tag{2}$$

have to be solved. Nevertheless, once the mesh motion is imposed, which is the main challenge for the computational flow modeling in a PCP, it can be extended for more complex flow situations.

Equation (1) becomes the constant volume constraint ($\nabla \cdot V=0$) for incompressible flow, but the equation is presented for the general case as is the form used in the discretization in CFX11. In the momentum conservation equation, $\mathbf{T}^{Turb}$ represents the turbulent stress tensor. Nevertheless, as will be shown in results section, several cases considering medium to high viscosity fluids, can be modeled considering laminar flow. For the case of low viscosity fluids, as water, the Eddy Viscosity Transport model, which is derived from k-ε model (Menter (1997)), was used. This model solves only one transport equation for the eddy viscosity. Although it provided good results, the effects of turbulence modeling on calculations, for low viscosity fluids, are object of current research.

A moving mesh was used to represent the rotor motion. In order to maintain the conservativeness of the numerical method the fluid velocity relative to the mesh velocity is considered for calculating the mass and momentum fluxes at control volumes faces in the discretization of the convective terms. In addition, the mesh topology has to be maintained along the time. This means that the elements are not suppressed or added in the domain, as rotor approaches to o retreats from the stator. These facts give place to extremely large mesh element deformations.

The mesh generation process for the fluid domain in a PCP is a very difficult task, particularly, in regions near the sealing lines, because of the high aspect ratio of the resulting elements in this region. The mesh generation and the imposition of the mesh motion represented the main challenge for the computational model implementation. Several topologies were evaluated in order to get a full hexahedral mesh with good element "quality". Independently of the numerical definition of “quality” in a computational mesh, the concept is understood as, the highest the quality, the lower is the element linear and angular distortion, which is known to generate bad conditioned matrices in equation discretization process and so numerical instabilities. In the extreme cases this lead to solver failure. This is a common problem in numerical simulations with moving meshes; even having a good “initial mesh”, mesh motion could lead to highly distorted elements if some cares are not taken. The mesh topology should be such that allows large deformation of the elements, which happens along one revolution of the rotor as illustrated in Figure 4. .Note that distances between rotor and stator were exaggerated in the figure, in order to show the mesh elements. Actual clearances are much smaller. Even more, for the case of interference, a very fine mesh was placed between rotor and stator, under the hypothesis of the existence of a lubricating film, as shown in Figure 6. The mesh generation for case with low clearances and interference was only possible through the very careful "node-by-node" mesh generation process used in this work. The details of the mesh generation algorithm are presented in Lima *et al.* (2009).

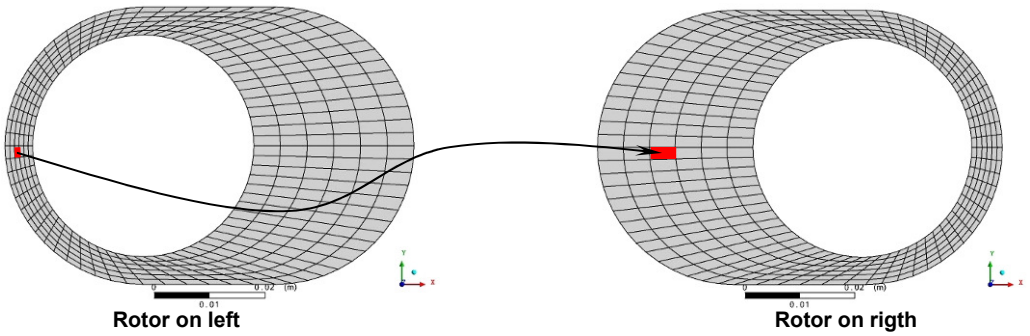

Figure 4. Element deformation in a transversal plane

Another difficulty for the model implementation was the imposition of mesh motion. As an initial approach, after good quality initial mesh was generated, simulations were performed by imposing the mesh motion directly on the solver used for simulations (CFX11). In this approach, the rotor wall motion is imposed, i.e., the wall nodes position are specified for each timestep, and the new positions of the internal nodes are calculated considering a linear elastic deformation of the mesh, by solving a Poisson equation for each coordinate (see ANSYS, 2008). The problem observed with this approach is that, due to the effects of numerical diffusivity on the calculation of mesh motion (internal nodes) an hysteresis-like process comes out leading to element distortion along rotor revolutions and the consequent solver failure due to element distortion after some revolutions of the rotor. The meshes for the same rotor position at two subsequent revolutions are shown in Figure 5.

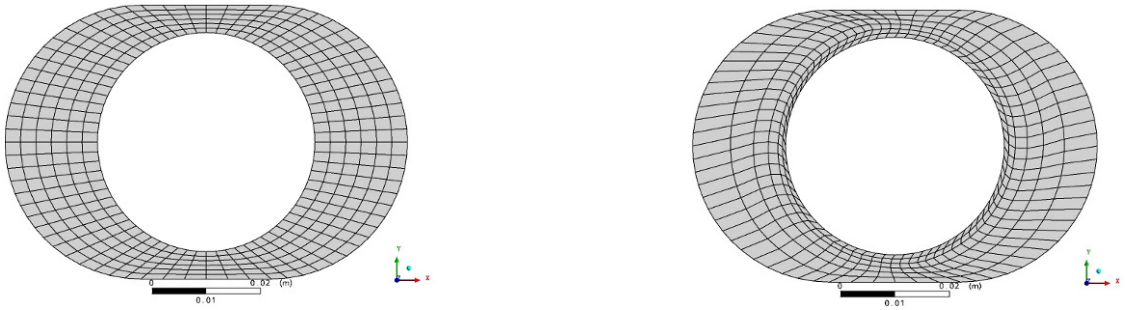

Mesh for initial time step **Mesh for time step corresponding to half a revolution**

Figure 5. Element distortion due to numerical diffusivity on the mesh motion calculation

The alternative used to impose the mesh motion was to specify each node position for each position of the rotor. This was accomplished by generating the mesh for each rotor position, and mapping the nodes bi-univocally from one time step to the next, maintaining the mesh topology.

This mesh generation for each rotor position and node mapping is defined through a FORTRAN user routines in CFX11 solver (ANSYS, 2008). Details of mesh generation process and mesh motion set-up are presented in Lima *et al.* (2009) and Lima & Paladino (2008). Snapshots of the computational meshes for different rotor positions are shown in Figure 6. As mesh is generated through a very careful process in which the position of the nodes is exactly defined node by node. Therefore, the use of double precision in mesh generation and numerical calculation allows the definition of extremely fine "channels" (about 1μm) for sealing region, with good quality elements.

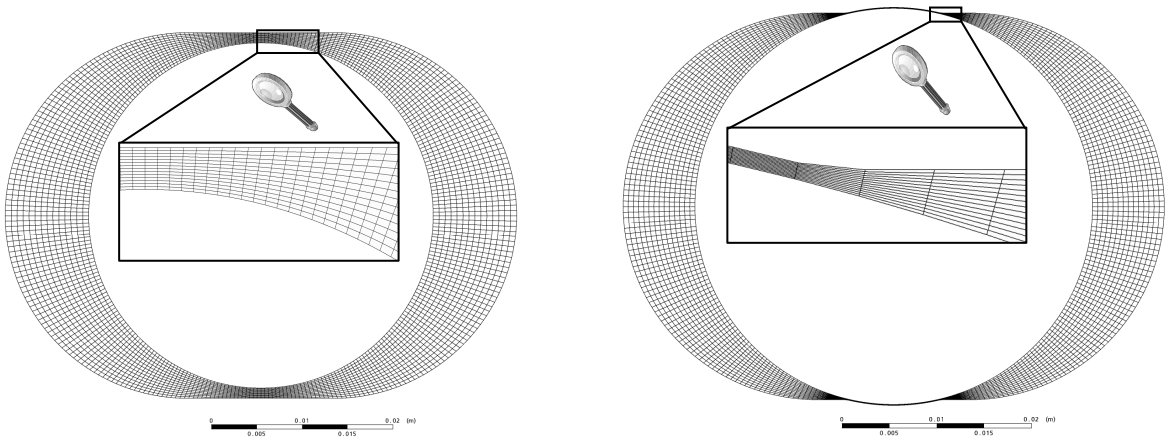

(a) (b)

Figure 6. Snapshots computational meshes for different rotor positions. (a) geometry with clearance and (b) geometry with interference

To impose the mesh motion each node position was specified for each position of the rotor along time. In order to maintain the conservativeness of the numerical method used for equations discretization in CFX11, only the coordinates of mesh nodes may change; and the topology or "connectivity" must remain fixed. To do this, a bi-univocal mapping has to be imposed between nodes of meshes for subsequent timesteps. The mesh topology is mapped at initial time, and the node coordinates are updated for subsequent timesteps. This process is defined through a FORTRAN user routine in CFX11 solver (ANSYS, 2008).

Model boundary conditions are depicted in Figure 7. Constant pressure averaged over the inlet (suction) and oultlet (discharge) regions, was imposed, and a rotating wall was considered for the rotor. Note that this condition represents the tangential velocity component of the rotor wall due to the rotation. The velocity component due to the rotor displacement, is naturally imposed by the mesh motion. Zero velocity conditions were imposed at stator.

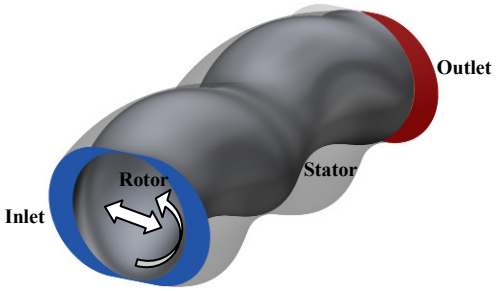

Figure 7. Model boundary conditions

3. MODEL VALIDATION AND RESULTS

In order to validate the fluid flow model, experimental results for a rigid stator (metallic) PCP, were used for comparison. This avoided to solve the stator deformation problem, which should be coupled through a Fluid-Structure-Interaction algorithm. For the case of elastomeric stator PCP, this coupling is very strong, as even small stator deformations, have important influence on the flow across seal lines. However, it is emphasized that the model developed is capable to deal with PCPs operating with interference between rotor and stator, since model for the stator deformation be included. Furthermore, the fluid model provides the pressure fields at stator wall, which is needed for stator deformation computation.

The model implemented was validated against Gamboa *et al.* (2002) and Gamboa *et al.* (2003) experimental results. Geometrical parameters of the PCP used in experiments developed by Gamboa *et al.* (2002) and Gamboa *et al.* (2003) are presented in Table 1.

Table 1. Geometrical parameters of the pump used in Gamboa`s experiments

Eccentricity – **E**	**4,039 mm**
Rotor Diameter– $\mathbf{d_R}$	**39,878 mm**
Stator Diameter – $\mathbf{d_S}$	**40,248 mm**
Clearance	**0,185 mm**
Stator Pitch	**119,990 mm**
Number of Stator Pitches	**3**

Results were validated for oil with dynamic viscosities of 42 cP and 481 cP and water. Volumetric flow rate versus total differential pressure for oil, are shown in Figure 8, compared with experimental results, for different pump rotation velocities.

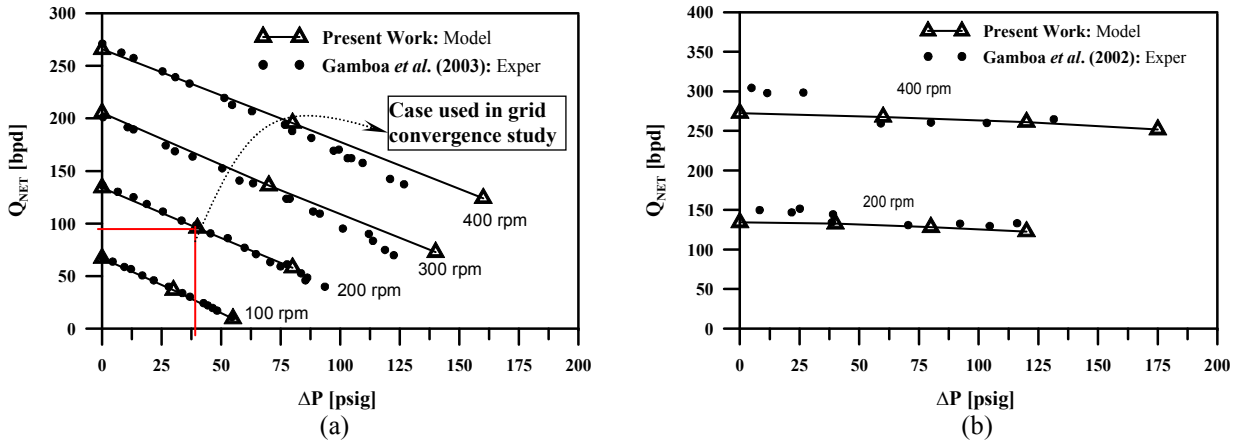

Figure 8. Flow rate versus differential pressure, for different rotation velocities, compared with experimental results for oil flow. (a) $\mu = 42$ cP and (b) $\mu = 481$ cP

Results shown in Figure 8 were calculated using a of 662200 nodes computational mesh. In order to optimize the computational time, and because of the observed sensitivity of the results to the mesh size, a mesh refinement study was performed. A case was selected, for a rotation velocity of 200 rpm, 42 cP viscosity oil and differential pressure of 40 psi. The case is indicated in Figure 8 (a). The calculated mass flow rate and torque versus mesh size are plotted in

Figure 9. The experimental value for mass flow rate is indicated as a reference. Unfortunately there were not found experimental values for torque in literature.

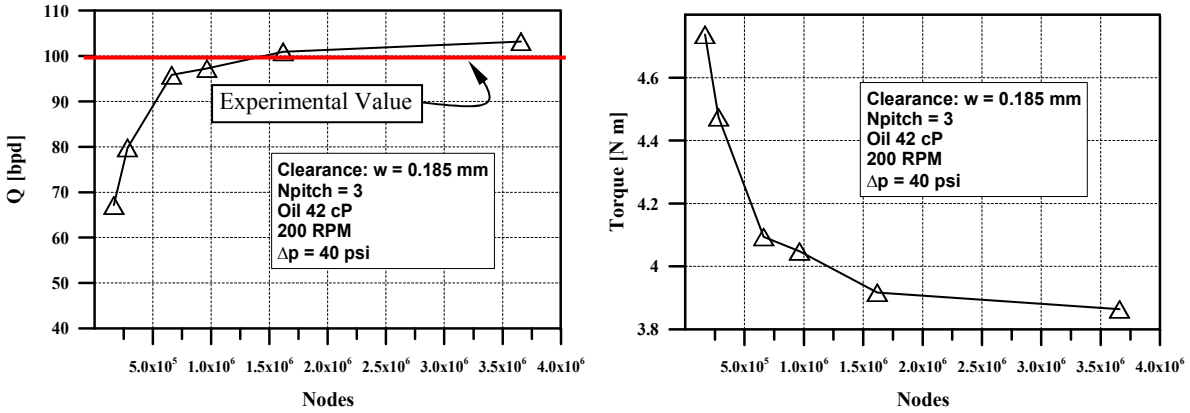

Figure 9. Grid convergence study for a case selected

For meshes above 1.5 million nodes, a small variations of mass flow rates can be observed. Values calculated for flow rate slightly over predicts the experimental value. Nevertheless, values obtained with grids form 662,000 to 3,658,200 nodes are in a range of 8bdp (95 and 103 bpd, respectively) and over prediction can be attributed to some differences in pump geometrical parameters used in experiments and simulations. Specifically, some uncertainties can be attributed to the measurement of the value of the clearance (Gamboa (2008), personal communication) which has a tremendous impact on slippage. In addition, only the pumping section is considered in the model, while the pressured drop in experiments is measured along the whole pump, including suction and discharge sections.

For the case of torque, results shows to be more sensitive to mesh size. This is a known fact for rotating machinery flow simulation, as viscous components of torque depends of wall viscous stresses which need a good near wall mesh refinement for accurate computation.

In terms of CPU requirements, the flow computation using a mesh of about 1e6 nodes, which provides good results for the conditions evaluated, require about 2 GB of RAM memory and takes about 48 hours in an Intel Centrino T9300, 2,5 GHz for oil flow and about 100 hours for water flow. This is because, as inertial terms become important for low viscosity, high density fluids, the number of internal timestep iterations required is higher (recalling that CFX11 solves mass and momentum equations in a coupled way and iterations are only required for coefficient update of convective terms in momentum equations). In addition a higher simulation time is required to attain a steady (periodic) state. Based on these facts it is important to make clear that CPU requirements strongly depend on conditions to be simulated and cannot be compared with requirements for simplified models. The model herby presented intends to provide information about PCP fluid dynamics which is not available from simplified approaches.

Results for water flow are shown in Figure 8. A mesh of 992,000 nodes was used in this case as results for water flow showed to be more sensitive to mesh size and a more reined grid was necessary to get results close to experimental values. This can be attributed to the higher relative importance of inertial terms in momentum balance, which requires finer meshes to reduce discretization errors. Although, model results are close to experiments, tendencies are still not satisfactory and this fact can be associated to the turbulence modeling. A study of the effects of turbulence modeling as well as mesh refinement for low viscosity fluids flow, is under run.

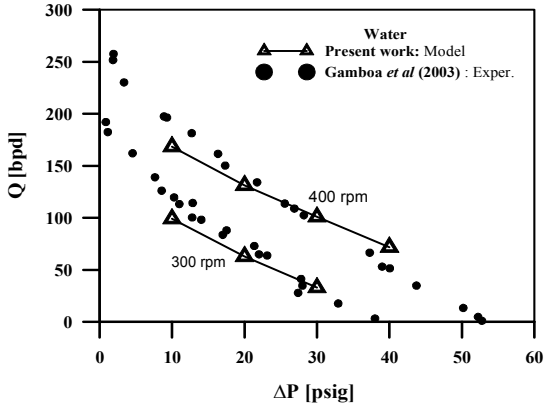

Figure 10. Flow rate versus differential pressure, for different rotation velocities, compared with experimental results for water flow.

3.1 Local and transient pressure distributions

Figure 11 presents the transient pressure variation during one revolution of the rotor, at a point located at the stator wall of the pump (shown in side figure), for oil and water flow. Pressure values are normalized by the total pressure drop along the pump. For the case of water flow (lower viscosity and higher density) inertial effects are important and a strong acceleration is experienced along seal lines, with the consequent pressure reduction. These effects can also be seen in pressure plot along a line (shown in yellow color in the side figure) located between rotor and stator, for a fixed time, shown in Figure 12. In Figure 13, snapshots of pressure contours for water flow, for different rotor positions are presented.

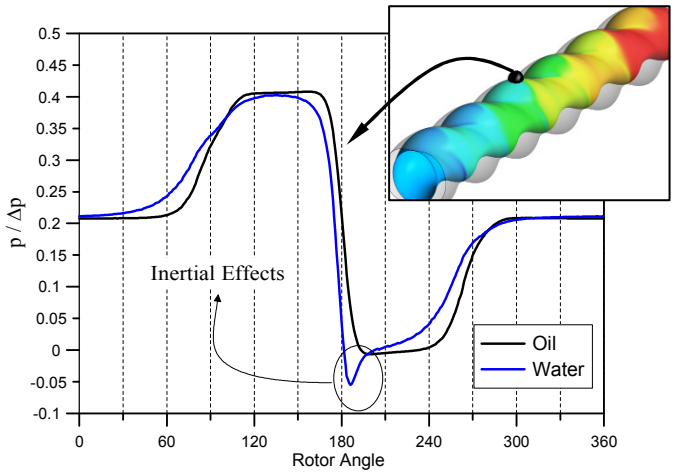

Figure 11. Pressure variation at stator wall, along on rotation of the rotor

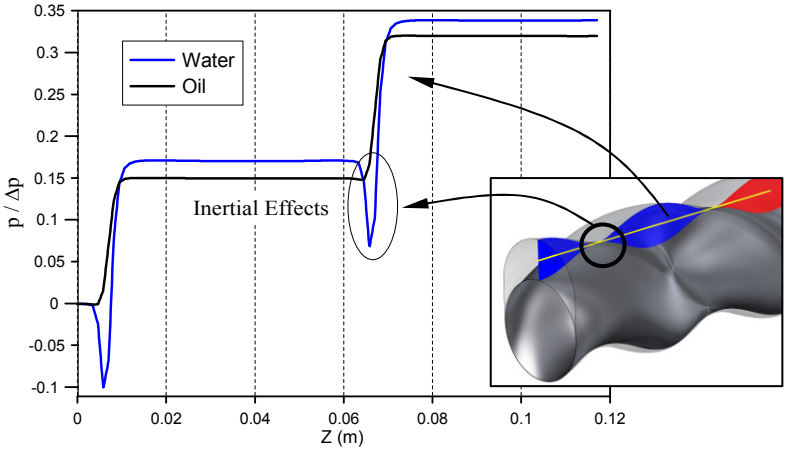

Figure 12. Pressure distribution along a line

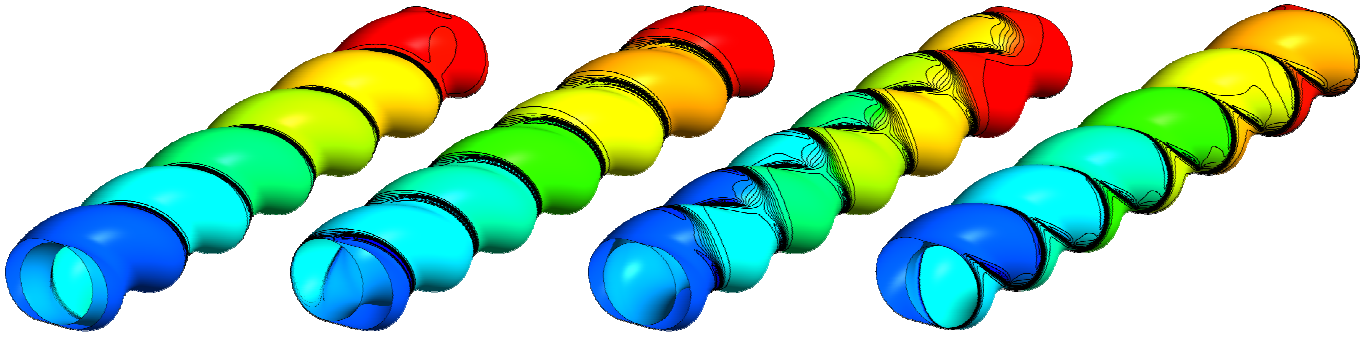

(0°) (90°) (180°) (270°)

Figure 13. Pressure contours along the pump stator

3.2 Hydraulic looses and efficiency

Once the implemented model provide all flow data, as pressure and velocity fields, the pump efficiency, including viscous looses, can be calculated. The isentropic efficiency for a pump is defined as

$$\eta_S = \frac{\dot{W}_{theroetical}}{\dot{W}_{real}} \tag{3}$$

where,

$$\dot{W}_{theroetical} = \Delta p\, \dot{V} \qquad \text{and} \qquad \dot{W}_{real} = T_z\, \omega_z \tag{4}$$

In the above equations, $\dot{V}$ T_z and ω are respectively, the volumetric flow rate, and the torque and rotation velocity along the axial direction. The equation for the theoretical work corresponds to the incompressible flow case. Note that the volumetric flow in eq. (4) corresponds to the actual flow rate pumped **not** the displaced volumetric flow rate. In posses of pressure and velocity fields, the torque over the rotor can be calculated as,

$$\vec{T} = \iint_{\substack{Rotor \\ Surface}} \left[p\vec{r} \times \overrightarrow{dA} + \overline{\overline{\tau}}_{visc} \cdot \vec{r} \times \overrightarrow{dA} \right] \tag{5}$$

The viscous stresses are calculated as function of velocities. For the case o turbulent flow, this includes both, viscous and turbulent stress tensors.

Torque and efficiency values for different fluids and operational conditions are presented in . Unfortunately no experimental results of torque and/or thermodynamic efficiency were found in literature to be used for comparison.

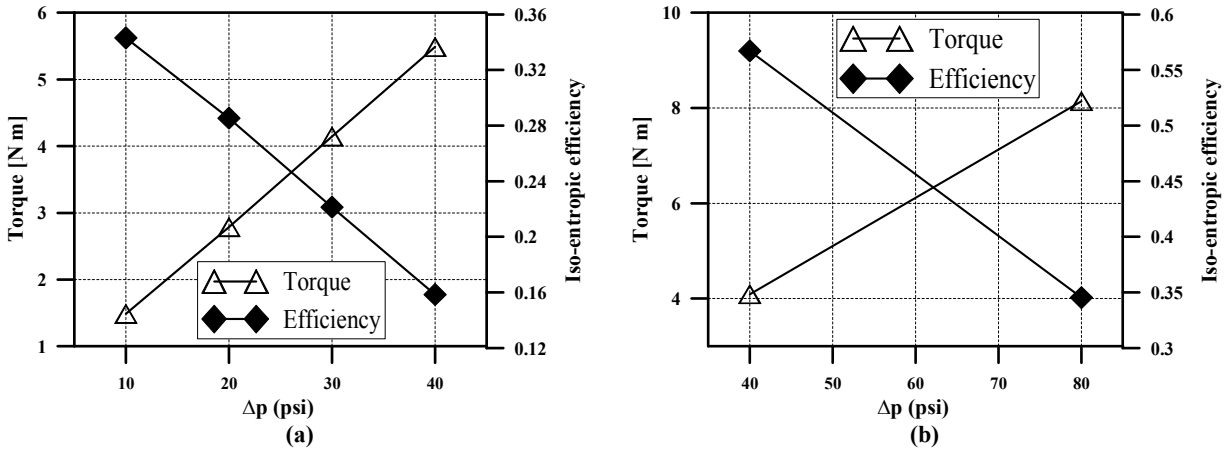

Figure 14. PCP Torque and efficiency versus Δp for (a) water and (b) oil, 42 cP

Efficiencies for oil are larger as slippage is lower. It is interesting to note that, although, the higher the viscosity, the higher the viscous losses, the pump present lower efficiencies for lower viscosity fluids. This is because a fixed amount of power is spent to displace fluid against a Δp but part of the displaced fluid returns back. Then as viscosity decrease, a larger part of the displaced flow rate returns and the power consumed for a specified flow rate pumped is larger. Values for efficiency were not validated against experiments. Then, although tendencies leading to the previous conclusion are reliable, actual values of efficiency strongly depend on mesh refinement. Note that flow rate and torque are on numerator and denominator in eq. (3), and then errors are magnified in efficiency calculation.

It is important to note that the efficiency given in eq. (3) is related to the power consumption for a given volumetric flow rate pumped and pressure difference along the pump. A more common design parameter of PCP systems is the volumetric efficiency which is usually determined from simplified models. This parameter can be easily calculated dividing the pumped volumetric flow rate by the displaced (theoretical) flow rate. Nevertheless, simplified models based on Mouneau`s approach do not allow to determine forces, torque and other important parameters for PCP systems design and operation, which usually need to be determined experimentally.

4. FINAL REMARKS

A detailed tridimensional computational model for the flow within a PCP, considering the rotor motion, was successfully implemented.

This model can provide detailed information about the pump performance for different geometrical parameters and operation conditions and represents the first attempt, at least in literature reviewed, for a complete flow simulation in real pump geometry, considering the rotor motion.

Besides the flow rate versus differential pressure, which is the most common design parameter and can be estimated using simplified approaches, detailed pressure and velocity fields result from the model. This information allow the calculation of other parameters as torque, forces and thermodynamic efficiency, which can de important in PCP system design operation and control.

Detailed pressure fields available allow the development of fluid-structure interaction models which could contemplate the elastomeric stator case. In addition, this model, based on the full solution of the Navier-Stokes equations within the PCP, can be extended for multiphase flow, which is the most common situation in oil field applications, using an Euelrian-Euelerian approach.

Results obtained are consistent with experimental results from literature but are very sensitive to the mesh size used for discretization. For the case of low viscosity fluids, some discrepancies are observed and will be subject of further investigations. These discrepancies are assumed to be due to turbulence modeling and investigations of turbulence modeling are in progress.

5. ACKNOWLEDGEMENTS

Authors are grateful to CENPES, UN-RNCE/PETROBRAS and PRH 14-ANP for the financial support of the present research.

6. REFERENCES

ANSYS CFX 11.0 Theory Manual (2008), ANSYS Inc., Cannonsbourg, PA, USA

Andrade, S. F., 2008, "Modelo Assintótico Para Escoamento Monofásico Em Bomba De Cavidade Progressiva , Pontificia Universidade Catoloca do Rio de Janeiro - PUC-Rio (in Portuguese).

Baliga, B. R. and Patankar, S. V., (1980), "A New Finite Element Formulation for Convection-Diffusion Problems", Numerical Heat Transfer, Vol. 3, pp 393-409.

Ferziger, J. H. & Peric, M., 2001, "Computational Methods for Fluid Dynamics", Springer-Verlag, 3rd Edition.

Gamboa, J.; Olivet, J.; Espin, S., 2003,"New Approach for Modelling Progressive Cavity Pumps Performance", Proceedings of SPE Annual Technical Conference and Exhibition, Denver, Colorado, USA.

Gamboa, J.; Olivet, J.; Iglesias, J.; Gonzalez, P., 2002, "Understanding the Performance of a Progressive Cavity Pump With a Metallic Stator", Proceedings of 20th International Pump Users Symposium.

ISO, 2008, "Downhole Equipment for Petroleum and Natural Gas Industries - Progressing Cavity Pump Systems for Artificial Lift", Technical Standards

Lima, J. A. and Paladino, E. E., 2008),"Simulação Computacional da Interação Fluido-Estrutura no Interior de Bombas de Cavidades Progressivas", Report No: 5

Lima, J. A.; Paladino, E. E.; Almeida, R. F., 2009,"Mesh Generation Process for the Numerical Simulation of the Fluid Structure Interaction, within Progressing Cavity Pumps", Proceedings of Brazilian Congress of Mechanical Engineering - COBEM 2009, Gramado, Nov. 15-20 (submitted).

Maliska, C. R., 2004, "Transferência De Calor e Mecânica Dos Fluidos Computacional (in Portuguese)", LTC Editora, 2nd Edition.

Menter, F. R., 1997, "Eddy Viscosity Transport Equations and Their Relation to the Model", ASME J.Fluids Engineering, Vol. 119, pp 876-884.

Moineau, R., 1930, "Le Noveau Capsulism", PhD Thesis, University of Paris, Paris.

Nelik, L. & Brennan, J., 2005, "Progressing Cavity Pumps, Downhole Pumps, and Mudmotors", Gulf Publishing Company, Houston, TX

Olivet, J.; Gamboa, J.; Kenyery, F., 2002,"Experimental Study of Two-Phase Pumping in a Progressive Cavity Pump Metal to Metal" Proceedings of SPE Annual Technical Conference and Exhibition, San Antonio, Texas, SPE 77730.

Raw, M. J., 1985, "A New Control-Volume-Based Finite Element Procedure for Numerical Solution of the Fluid Flow and Scalar Transport Equations" , University of Waterloo, Canada.

Robello, S. G. & Saveth, K., 1998, "Progressing Cavity Pump (PCP): New Performance Equations for Optimal Design", Proceedings of SPE Permian Basin Oil and Gas Recovery Conference, Midland, Texas, US, SPE 39786.

7. RESPONSIBILITY NOTICE

The authors are the only responsible for the printed material included in this paper.